

Supplementary Material:

Impact of phases distribution on mixing and reactions in unsaturated porous media

Joaquín Jiménez-Martínez^{1,2*}, Andrés Alcolea³, Julien A. Straubhaar⁴, Philippe Renard⁴

¹*Department of Water Resources and Drinking Water, EAWAG, 8600 Dübendorf, Switzerland.*

²*Department of Civil, Environmental and Geomatic Engineering, ETH Zurich, 8093 Zürich, Switzerland.*

³*HydroGeoModels AG, Tössstalstrasse 23, 8400 Winterthur, Switzerland.*

⁴*Centre d'Hydrogéologie et de Géothermie (CHYN), University of Neuchâtel, 2000 Neuchâtel, Switzerland.*

* Corresponding author: joaquin.jimenez@eawag.ch; jjimenez@ethz.ch

Figures:

Figure S1

Figure S2

Figure S3

Figure S4

Figure S5

Figure S6

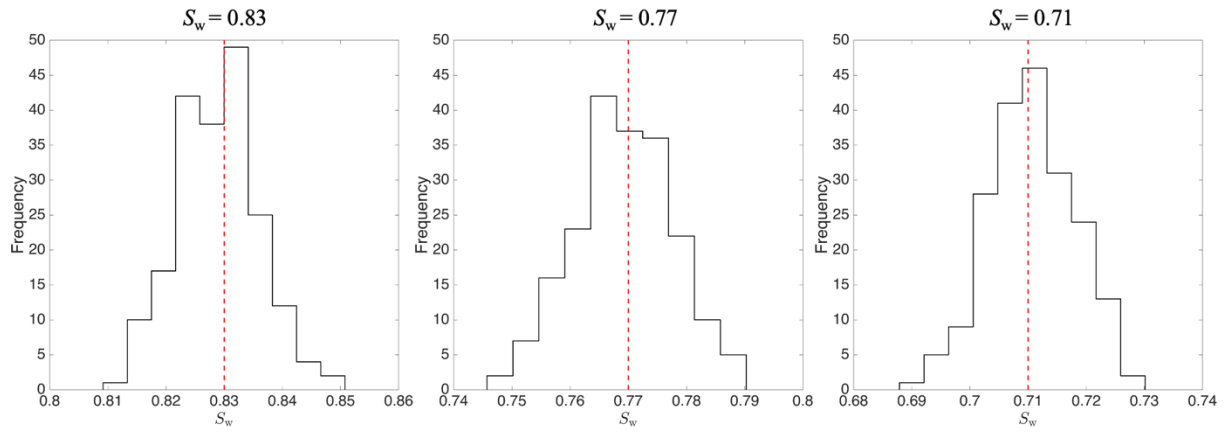


Figure S1. Histogram of the 200 simulated saturations for each TDS (blue). The saturation of the TDS is depicted by the vertical dashed line.

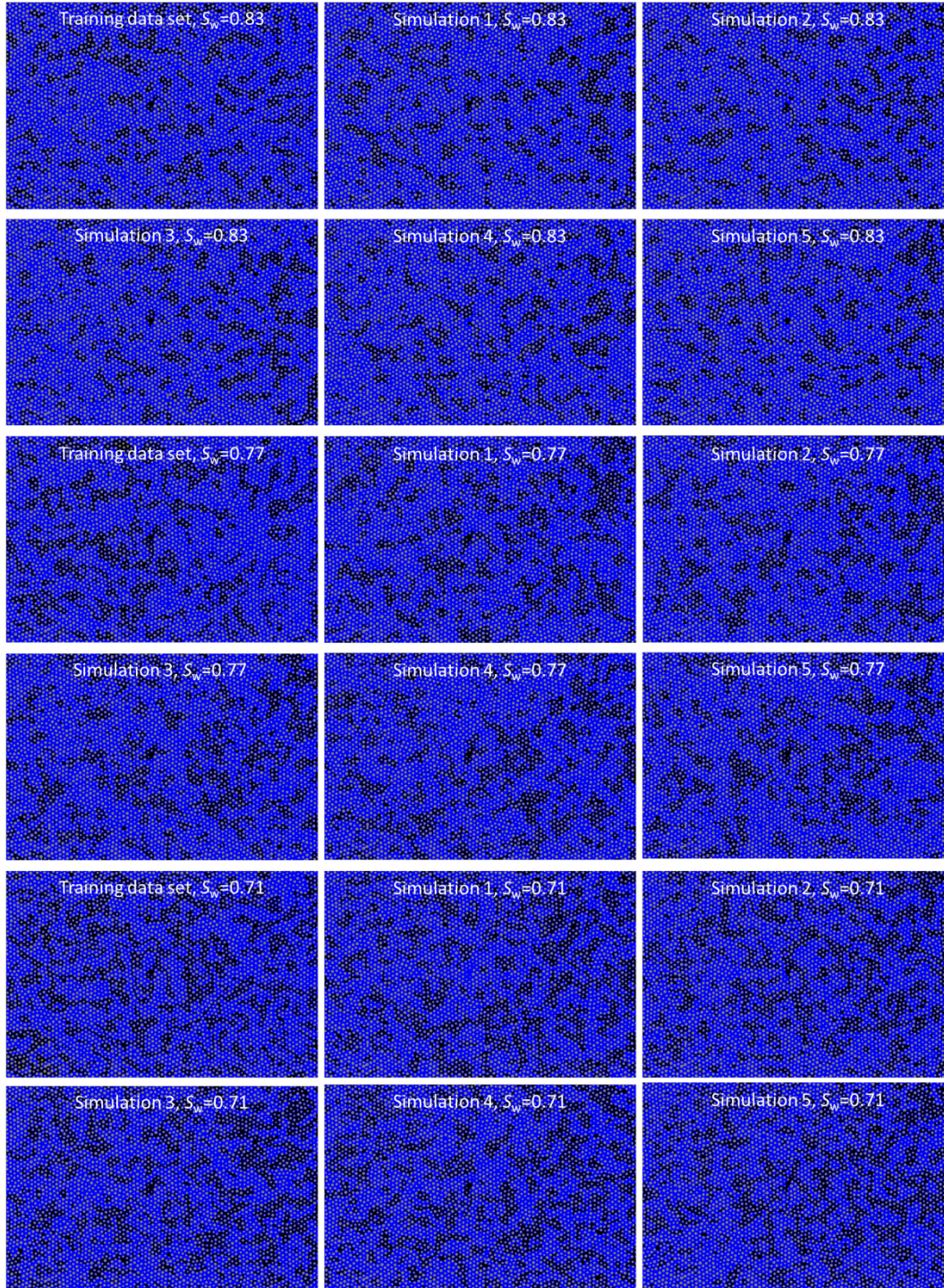


Figure S2. Training data sets and simulations. Non-wetting phases are air (clusters in black) and solid obstacles (in grey). The wetting phase (water) is depicted in blue.

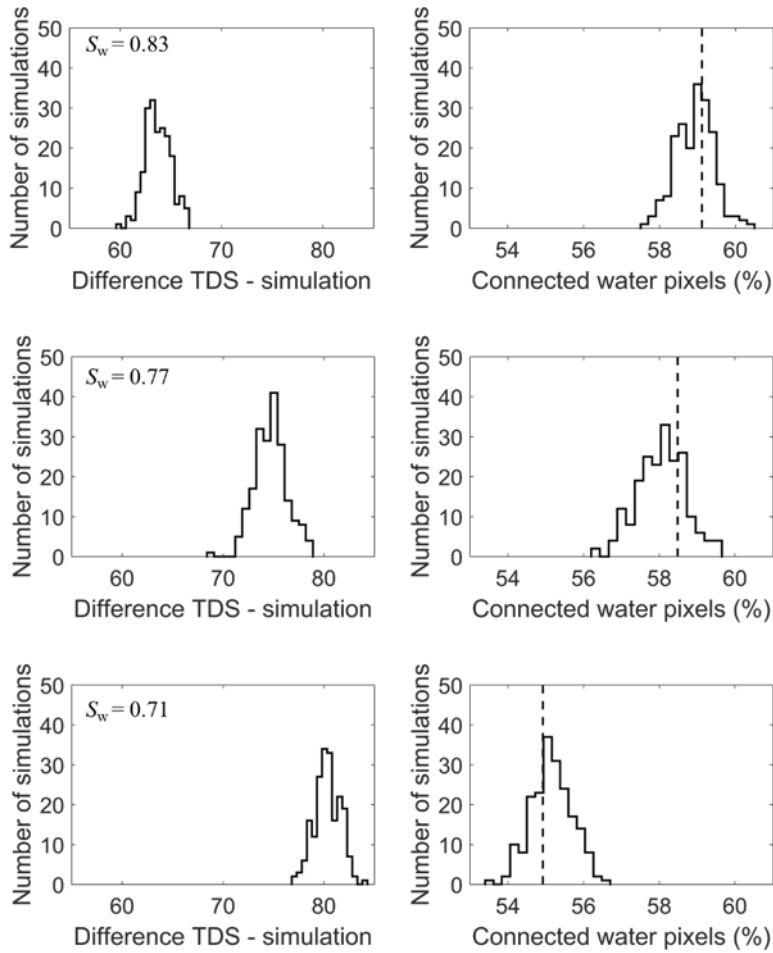


Figure S3. Similarity and dissimilarity measures between the TDS and the generated MPS simulations for different saturations (rows). The first column depicts the histogram of the fraction of non-solid pixels whose simulated value is different to that in the TDS (*e.g.*, air in the simulation but water in the TDS). The second column depicts the histogram of the proportion of the wet pixels that connect the inlet and the outlet of the domain in the simulations and in the TDS (dashed black line).

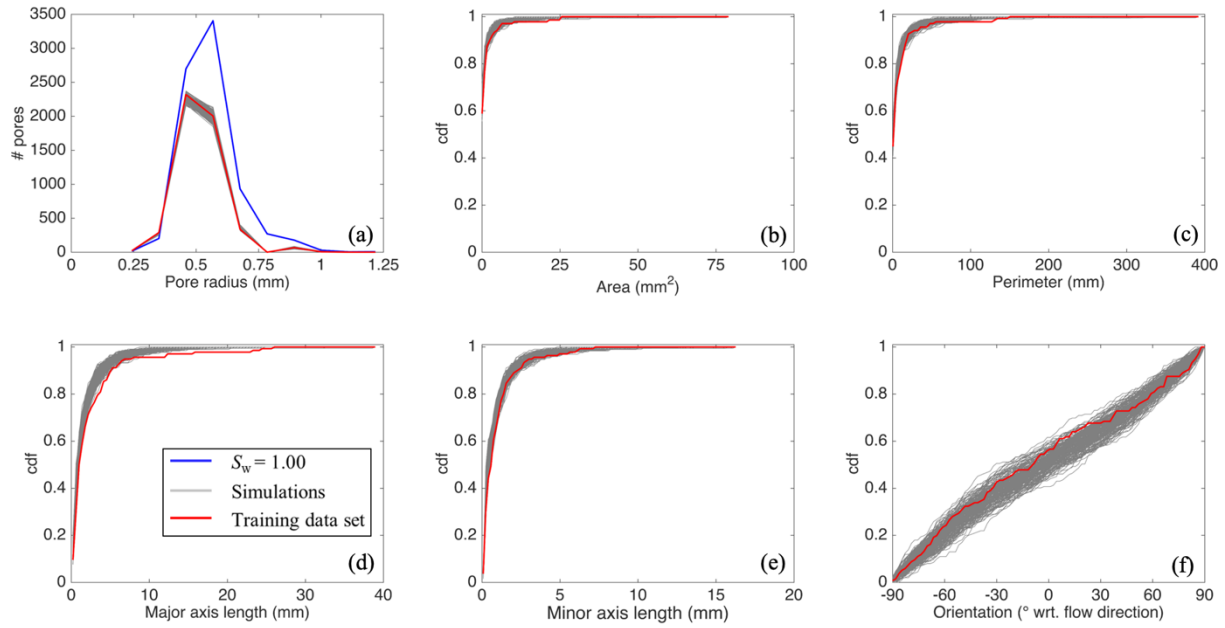


Figure S4. Comparison between geometric descriptors of the simulated distributions of air clusters (non-wetting phase; grey lines) and those of the training data set for a saturation $S_w = 0.77$ (red line): unsaturated pore radii (a), cumulative distribution function (cdf) of the area (b) and perimeter (c) of the air clusters, cdfs of the major (d) and minor (e) axes lengths of area-equivalent ellipses fitting the air clusters, and cdfs of the orientation of air clusters with respect to the main flow direction in the flow and transport model (f). The blue line in panel (a) represents $S_w = 1.00$ as a reference.

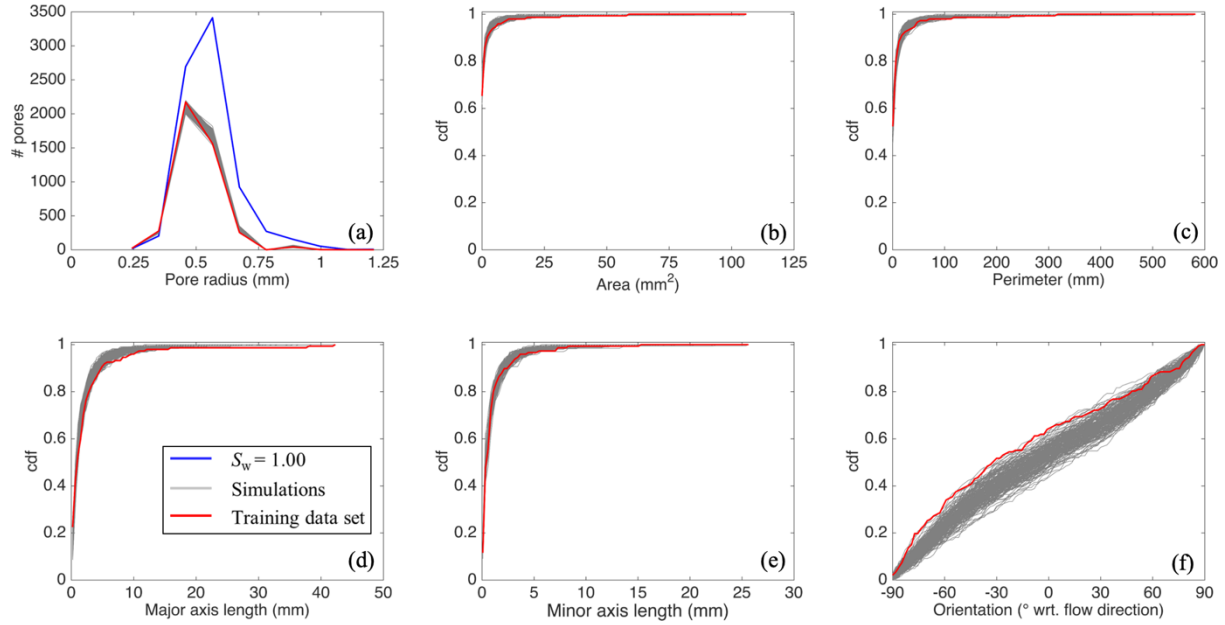


Figure S5. Comparison between geometric descriptors of the simulated distributions of air clusters (non-wetting phase; grey lines) and those of the training data set for a saturation $S_w = 0.71$ (red line): unsaturated pore radii (a), cumulative distribution function (cdf) of the area (b) and perimeter (c) of the air clusters, cdfs of the major (d) and minor (e) axes lengths of area-equivalent ellipses fitting the air clusters, and cdfs of the orientation of air clusters with respect to the main flow direction in the flow and transport model (f). The blue line in panel (a) represents $S_w = 1.00$ as a reference.

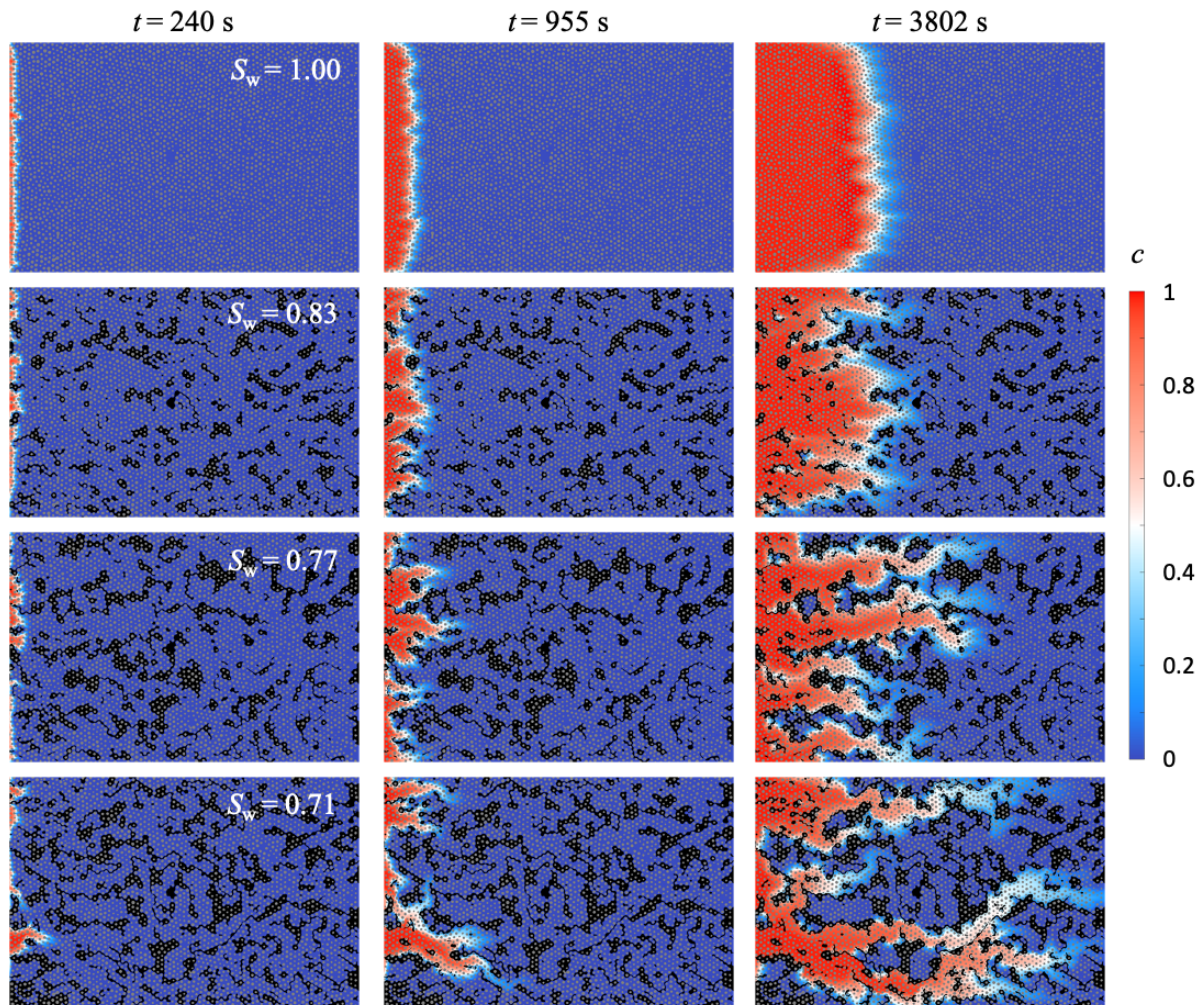


Figure S6. Spatial distribution of concentration (c) obtained under fully saturated ($S_w = 1.00$) and unsaturated conditions ($S_w = 0.83, 0.77,$ and 0.71) at common time steps, $t = 240, 955$ and 3802 s, using the training data set (air phase: black; solid obstacles: grey). Péclet numbers are reported in Table 1. As saturation decreases, high (preferential flow paths) and low (stagnation zones) velocity regions are created and differences between low and high velocities are incremented, which induces a larger deformation of the injected front.